

ORIGINAL ARTICLE

**Static Force Analysis of Foot of Electrically
Driven Heavy-Duty Six-Legged Robot
under Tripod Gait**

Communication author: Hong-Chao Zhuang

Email: zhuanghongchao_hit@163.com

mobile phone: +86-17702207680 QQ: 214922912

Contents

- 1 Introduction
- 2 Configuration and Typical Walking Mode of Robot
- 3 Static Analysis of Robot
- 4 Force Theoretical Analysis of Foot under Gait of Robot
- 5 Force Experimental Analysis of Foot under Robotic Gait
- 6 Conclusions

1 Introduction

- With the development of robotics, the autonomous mobile robot has been widely used. **Intelligent, high pass and large load-ratio robots** have been gradually regarded as an important developing factor for the engineering of mobile robots.
- The technology parameters of the heavy-duty multi-legged robots, such as **BigDog**, **Ambler**, **ATHLETE**, and **Dante II**, concludes that **the heavy-duty multi-legged robots have three major characteristics** comparing to the non-heavy-duty or small multi-legged robots; they are the **larger volume, bigger mass, and larger load-ratio**.
- The conventional gait of the six-legged robot involves a tripod gait, a tetrapod gait, and a five-legged gait. The **tripod gait** is the fastest and most common for the six-legged robots and hexapod.

1 Introduction

- The relationship between the gait and the normal force of foot will be important for reducing the power consumption of mobile systems and improving the load ratio and stability of heavy-duty multi-legged robots.
- Then, it can be found that many researchers mainly focus on the gait or force distribution for legged robots. There is less research on the relationship between the gait and the normal force of foot, especially for heavy-duty multi-legged robots

2 Configuration and Typical Walking Mode of Robot

2.1 Configuration of Robot

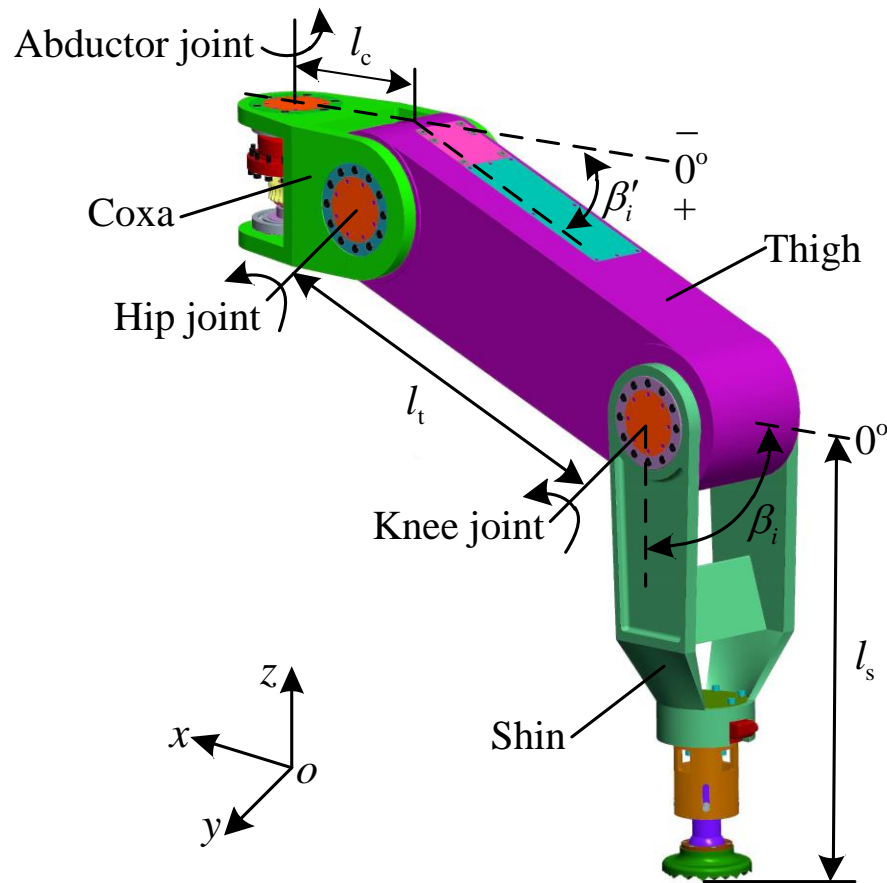


Fig. 1 Structure of single leg of heavy-duty six-legged robot

2 Configuration and Typical Walking Mode of Robot

2.1 Configuration of Robot

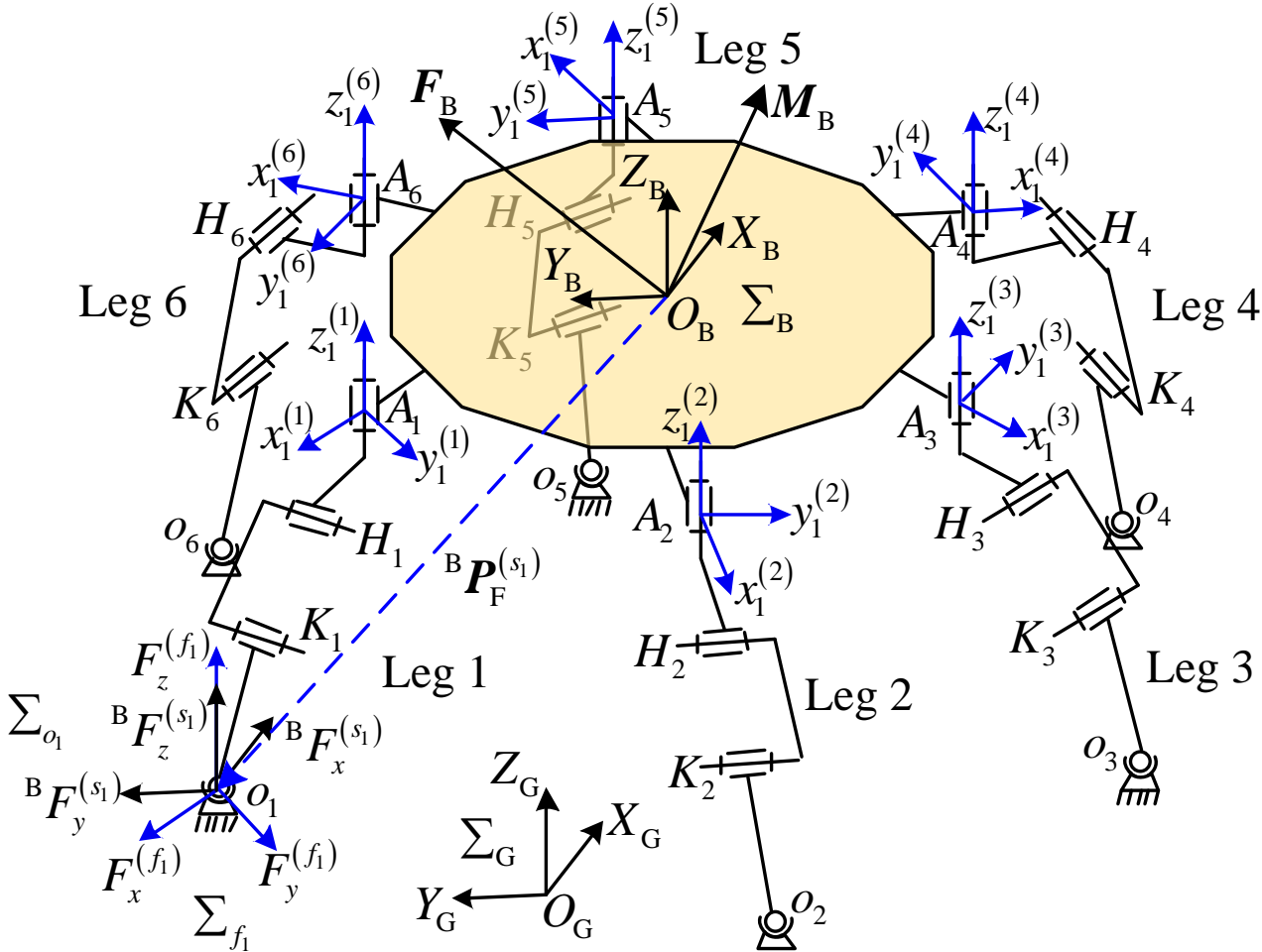


Fig. 2 Mechanism of heavy-duty six-legged robot

2 Configuration and Typical Walking Mode of Robot

2.1 Configuration of Robot

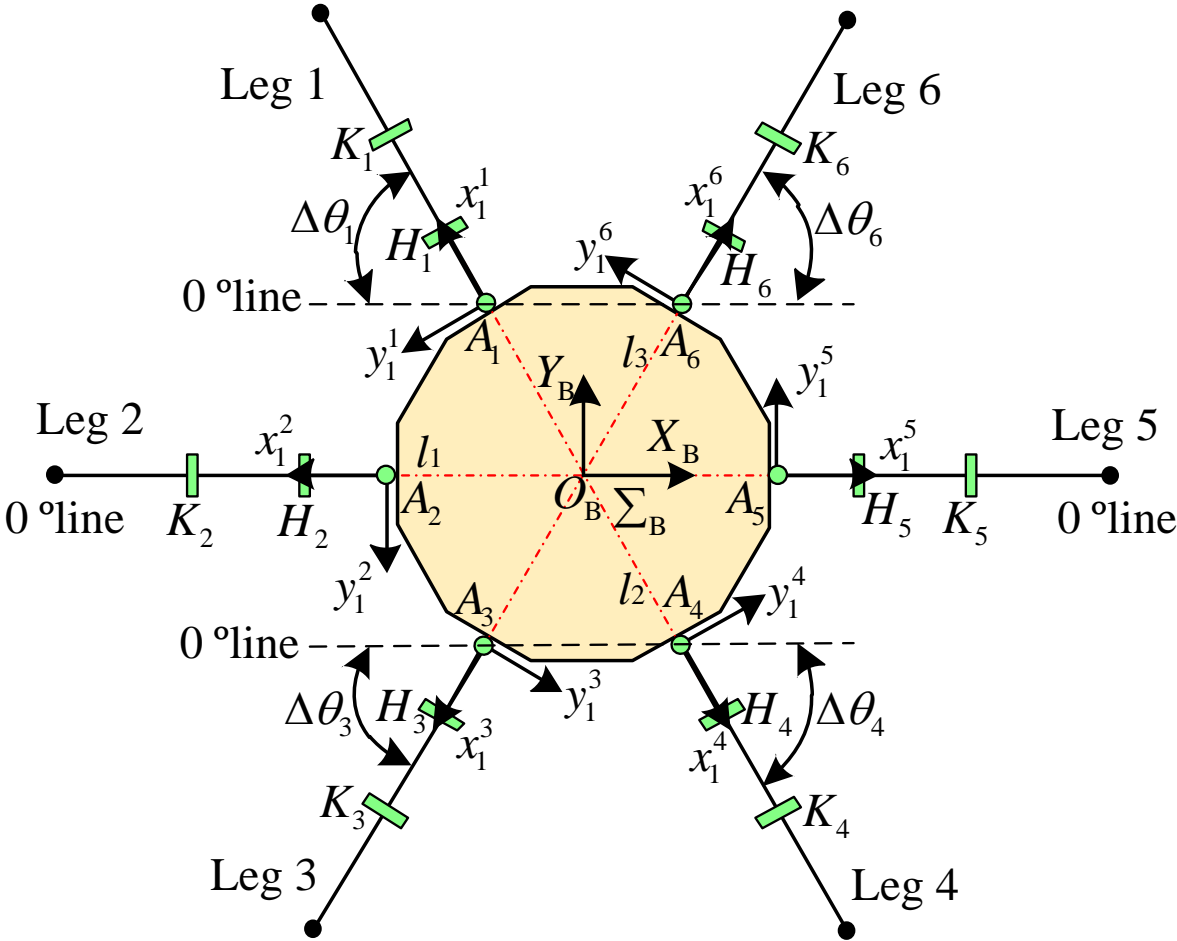


Fig. 3 Top view of mechanism of six-legged robot

2 Configuration and Typical Walking Mode of Robot

2.2 Typical Walking Mode of Robot

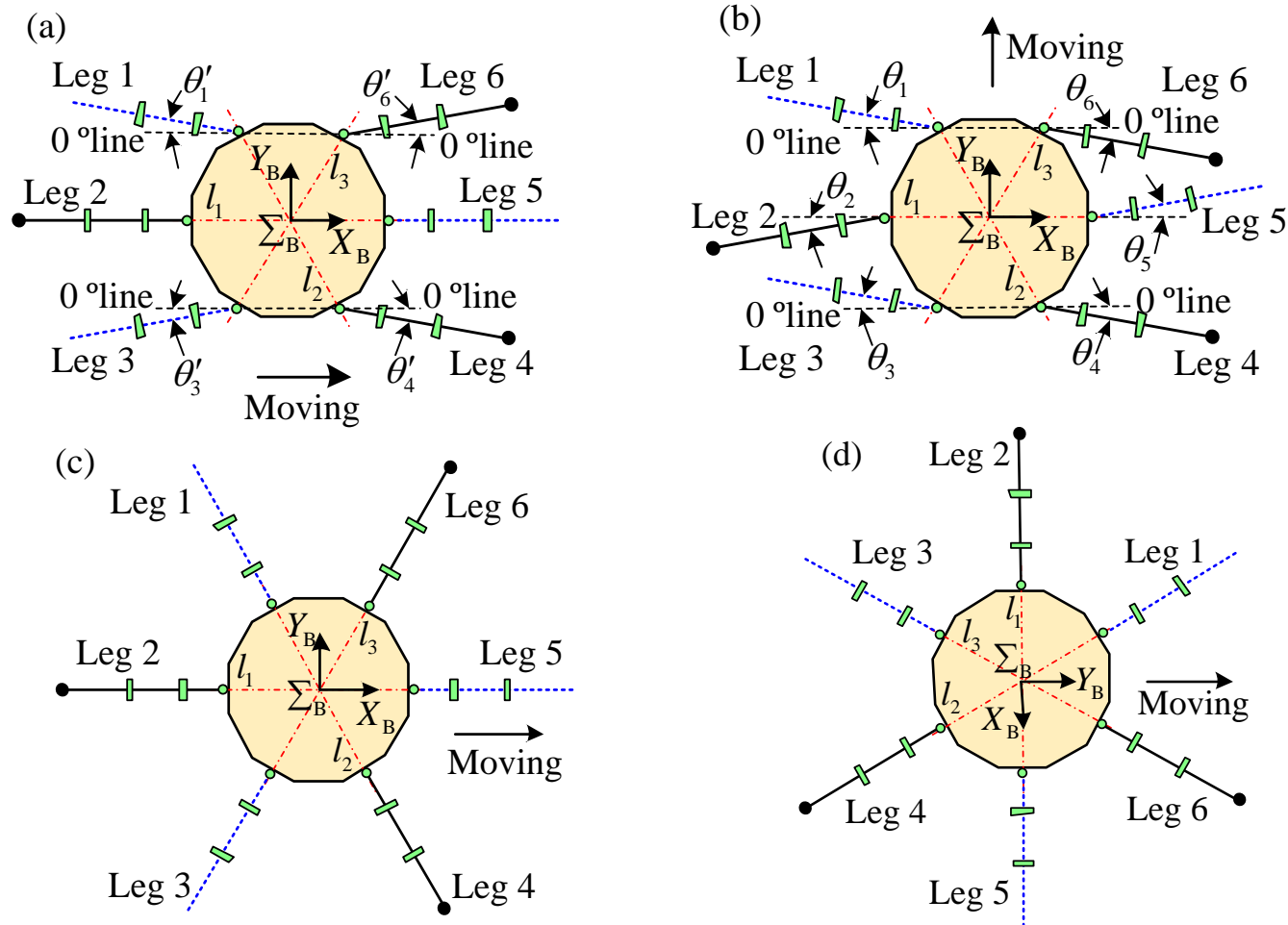


Fig. 4 Four kinds of typical tripod gaits of heavy-duty six-legged robot((a) Crab type; (b) Ant type; (c) Mixture type I; (d) Mixture type II)

3 Static Analysis of Robot

$$\sum_{k=1}^u {}^B \mathbf{F}_{s_k} = \mathbf{J}_F {}^B \mathbf{F}_s = \begin{pmatrix} 1 & 0 & 0 & \cdots & 1 & 0 & 0 \\ 0 & 1 & 0 & \cdots & 0 & 1 & 0 \\ 0 & 0 & 1 & \cdots & 0 & 0 & 1 \end{pmatrix} \begin{pmatrix} {}^B \mathbf{F}_x^{(s_1)} \\ {}^B \mathbf{F}_y^{(s_1)} \\ {}^B \mathbf{F}_z^{(s_1)} \\ \vdots \\ {}^B \mathbf{F}_x^{(s_u)} \\ {}^B \mathbf{F}_y^{(s_u)} \\ {}^B \mathbf{F}_z^{(s_u)} \end{pmatrix} = \mathbf{F}_B, \quad (3)$$

$$\mathbf{J}_M {}^B \mathbf{F}_s = \mathbf{M}_B \quad (4)$$



The equilibrium matrix of generalized force can be obtained for the support phase of robot as follows:

$$\hat{\mathbf{J}} {}^B \mathbf{F}_s = \begin{pmatrix} \mathbf{I}_{3 \times 3} & \mathbf{I}_{3 \times 3} & \cdots & \mathbf{I}_{3 \times 3} \\ {}^B \mathbf{P}_F^{(s_1)} & {}^B \mathbf{P}_F^{(s_2)} & \cdots & {}^B \mathbf{P}_F^{(s_u)} \end{pmatrix} \begin{pmatrix} {}^B \mathbf{F}_{s_1} \\ {}^B \mathbf{F}_{s_2} \\ \vdots \\ {}^B \mathbf{F}_{s_u} \end{pmatrix} = \begin{pmatrix} \mathbf{F}_B \\ \mathbf{M}_B \end{pmatrix} = \hat{\mathbf{A}}. \quad (5)$$

3 Static Analysis of Robot

The force of the foot is zero when the leg is in transfer phase:

$${}^B\mathbf{F}_t = \left({}^B\mathbf{F}_{t_1} \quad {}^B\mathbf{F}_{t_2} \quad \dots \quad {}^B\mathbf{F}_{t_e} \quad \dots \quad {}^B\mathbf{F}_{t_r} \right)^T = 0 \quad (6)$$



Based on Eqs. (5) and (6), the equilibrium matrix of general force can be written for the system of heavy-duty six-legged robot as follows:

$$\begin{pmatrix} \hat{\mathbf{J}} & \mathbf{O}_{6 \times 3r} \\ \mathbf{O}_{3r \times 3u} & \mathbf{I}_{3r \times 3r} \end{pmatrix} \begin{pmatrix} {}^B\mathbf{F}_s \\ {}^B\mathbf{F}_t \end{pmatrix} = \begin{pmatrix} \hat{\mathbf{A}} \\ \mathbf{0} \end{pmatrix} \quad (7)$$

4 Force Theoretical Analysis of Foot under Gait of Robot

When the tangential force of the foot is ignored, the expression can be obtained for the normal force of the foot in the support phase as follows:

$$\begin{pmatrix} {}^B \mathbf{F}_{s_2} \\ {}^B \mathbf{F}_{s_4} \\ {}^B \mathbf{F}_{s_6} \end{pmatrix}^T = \begin{pmatrix} 0 & 0 & {}^B F_z^{(s_2)} & 0 & 0 & {}^B F_z^{(s_4)} & 0 & 0 & {}^B F_z^{(s_6)} \end{pmatrix} \quad (10)$$

Based on Eq. (5), the equilibrium matrix of general forces in the support phase can be deduced for the heavy-duty six-legged robot as follows:

$$\hat{\mathbf{J}}^B \mathbf{F}_s = \begin{pmatrix} \mathbf{I}_{3 \times 3} & \mathbf{I}_{3 \times 3} & \mathbf{I}_{3 \times 3} \\ {}^B \mathbf{P}_F^{(s_2)} & {}^B \mathbf{P}_F^{(s_4)} & {}^B \mathbf{P}_F^{(s_6)} \end{pmatrix} \begin{pmatrix} {}^B \mathbf{F}_{s_2} \\ {}^B \mathbf{F}_{s_4} \\ {}^B \mathbf{F}_{s_6} \end{pmatrix} = \begin{pmatrix} \mathbf{F}_B \\ \mathbf{M}_B \end{pmatrix} \quad (11)$$

4 Force Theoretical Analysis of Foot under Gait of Robot

Eqs. (4), (9), and (10) are respectively substituted into Eq. (11), and the equilibrium equations of robot can be deduced as follows:

$$\left\{ \begin{array}{l} {}^B F_z^{(s_2)} + {}^B F_z^{(s_4)} + {}^B F_z^{(s_6)} = m_L g + m_R g \\ {}^B P_{Fy}^{(s_2)} {}^B F_z^{(s_2)} + {}^B P_{Fy}^{(s_4)} {}^B F_z^{(s_4)} + {}^B P_{Fy}^{(s_6)} {}^B F_z^{(s_6)} = 0 \\ {}^B P_{Fx}^{(s_2)} {}^B F_z^{(s_2)} + {}^B P_{Fx}^{(s_4)} {}^B F_z^{(s_4)} + {}^B P_{Fx}^{(s_6)} {}^B F_z^{(s_6)} = 0 \end{array} \right. \quad (12)$$

4 Force Theoretical Analysis of Foot under Gait of Robot

4.1 Theoretical Analysis of Normal Force of Foot under Ant-Type Tripod Gait

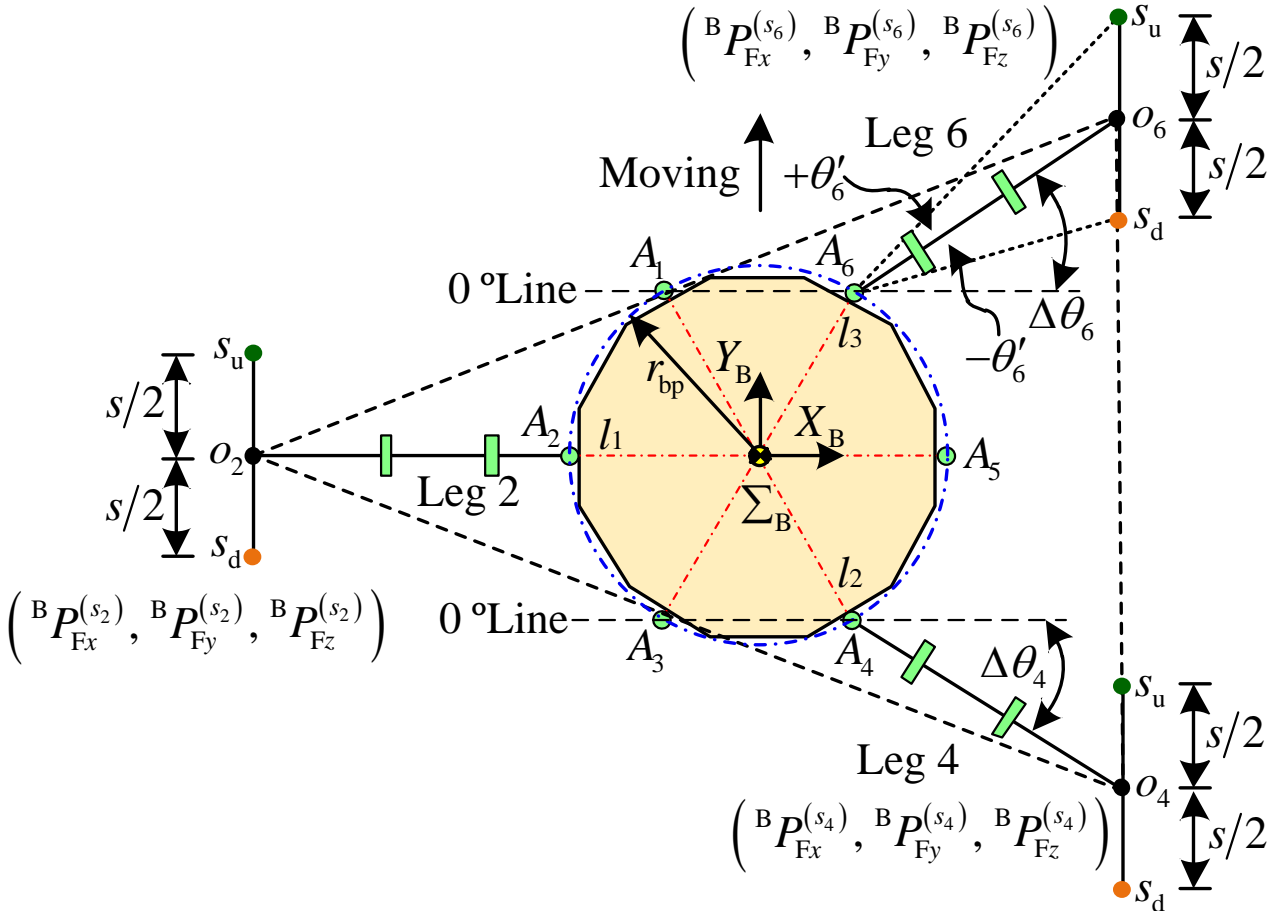


Fig. 5 Support phase of heavy-duty six-legged under ant-type tripod gait

4 Force Theoretical Analysis of Foot under Gait of Robot

4.1 Theoretical Analysis of Normal Force of Foot under Ant-Type Tripod Gait

Based on Fig. 5, the coordinates of the legs' feet in the support phase can be obtained along the x direction of the body coordinate system as follows:

$$\begin{cases} {}^B P_{Fx}^{(s_2)} = -(r_{bp} + L'_{P2}) \\ {}^B P_{Fx}^{(s_4)} = r_{bp} \cos 60^\circ + L'_{P4} \cos(\Delta\theta_4) \\ {}^B P_{Fx}^{(s_6)} = r_{bp} \cos 60^\circ + L'_{P6} \cos(\Delta\theta_6) \end{cases} \quad (14)$$

The coordinates of the feet at the lowest point sd can be respectively deduced along the y direction in the body coordinate system for legs 2, 4, and 6; they are shown as follows:

$$\begin{cases} {}^B P_{Fy}^{(s_2)} = -s/2 \\ {}^B P_{Fy}^{(s_4)} = -(r_{bp} \sin 60^\circ + L'_{P4} \sin(\Delta\theta_4)) - s/2 \\ {}^B P_{Fy}^{(s_6)} = (r_{bp} \sin 60^\circ + L'_{P6} \sin(\Delta\theta_6)) - s/2 \end{cases} \quad (15)$$

4 Force Theoretical Analysis of Foot under Gait of Robot

Eq. (14) and Eq. (15) can be substituted into Eq. (12). The mathematical models of the normal forces of feet can be respectively deduced for the legs 2, 4, and 6. Then

$$\left\{ \begin{array}{l} {}^B F_z^{(s_2)} = \frac{r_{bp} + 2L'_{PS} \cos(\Delta\theta)}{Q_3} (m_L g + m_R g) \\ {}^B F_z^{(s_4)} = \frac{Q_1 - Q_2}{Q_3 \times Q_4} (m_L g + m_R g) \\ {}^B F_z^{(s_6)} = \frac{Q_1 + Q_2}{Q_3 \times Q_4} (m_L g + m_R g) \end{array} \right. \quad (16)$$

where

$$\left\{ \begin{array}{l} Q_1 = (r_{bp} + L'_{PS}) (\sqrt{3}r_{bp} + 2L'_{PS} \sin(\Delta\theta)) \\ Q_2 = (3r_{bp}/2 + L'_{PS} + L'_{PS} \cos(\Delta\theta)) s \\ Q_3 = 3r_{bp} + 2L'_{PS} + 2L'_{PS} \cos(\Delta\theta) \\ Q_4 = \sqrt{3}r_{bp} + 2L'_{PS} \sin(\Delta\theta) \end{array} \right.$$

4 Force Theoretical Analysis of Foot under Gait of Robot

- The step pitch s , height h of body, and initial offset L'_{PS} are respectively set by 0.4 m, 0.5 m, and 0.68 m for the heavy-duty six-legged robot, when the feet in the support phase move from the upper point s_u to the lower point s_d .
- The ranges of the initial angles of the abductor joints are from 0° to 60° for legs 1, 3, 4, and 6. The radius r_{bp} of the body is introduced in Eq. (16).
- MATLAB software is used to compile programs for analyzing the normal forces of feet of the support phase under the ant-type tripod gait.
- The variable tendency charts of the normal forces of feet are obtained and respectively shown in Fig. 6, Fig. 7, and Fig. 8 for legs 2, 4, and 6.

4 Force Theoretical Analysis of Foot under Gait of Robot

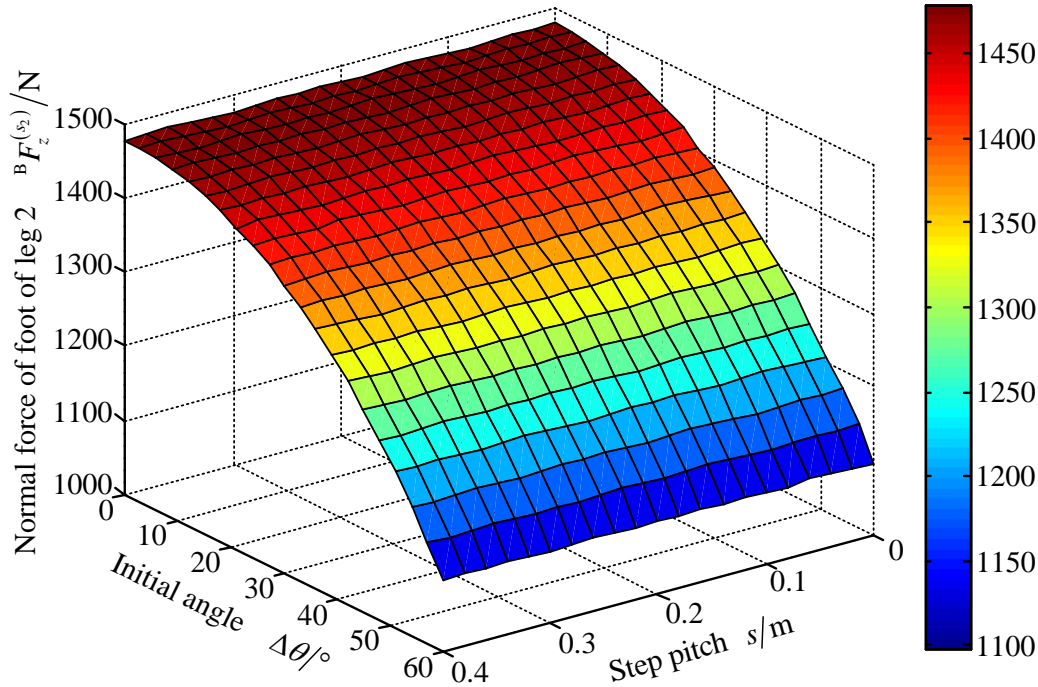


Fig. 6 Variable tendency chart of normal force of foot for leg 2 with changes in $\Delta\theta$ and s under ant-type tripod gait

- Based on Fig. 6, the normal force of the foot of leg 2 gradually decreases from 1478 N to 1098 N, when the initial angle $\Delta\theta$ of abductor joint varies from 0° to 60° .
- The normal force of the foot of leg 2 is a constant with a change of step pitch s .
- When the initial angle $\Delta\theta$ of the abductor joint is 20° , the normal force of the foot is about 1442 N for leg 2.

4 Force Theoretical Analysis of Foot under Gait of Robot

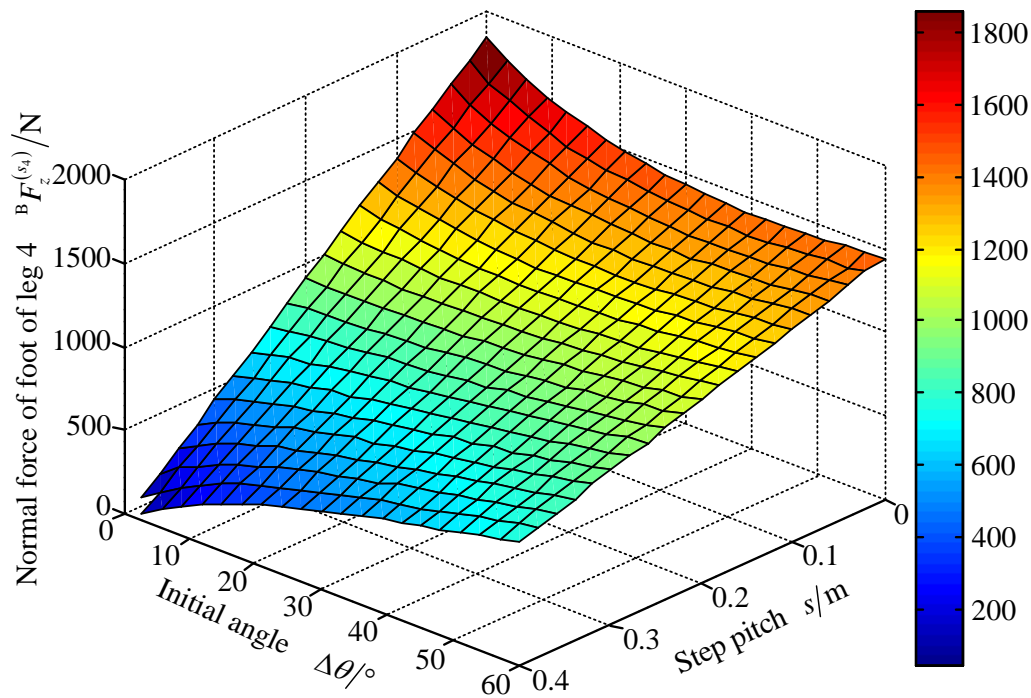


Fig. 7 Variable tendency chart of normal force of foot for leg 4 with changes in $\Delta\theta$ and s under ant-type tripod gait

- Based on Fig. 7, with the initial angle $\Delta\theta$ varying from 0° to 60° ; it shows that the variable tendency of the foot's normal force overall presents from augmentation to a decrease for the leg 4, when the step pitch s is between 0 m to 0.2 m.
- The normal force of the foot of leg 4 gradually increases when the step pitch s is between 0.2 m to 0.4 m.
- It also shows that the normal force of the foot overall decreases for leg 4, when the initial angle $\Delta\theta$ is a fixed value and the range of step pitch s is from 0 m to 0.4 m.

4 Force Theoretical Analysis of Foot under Gait of Robot

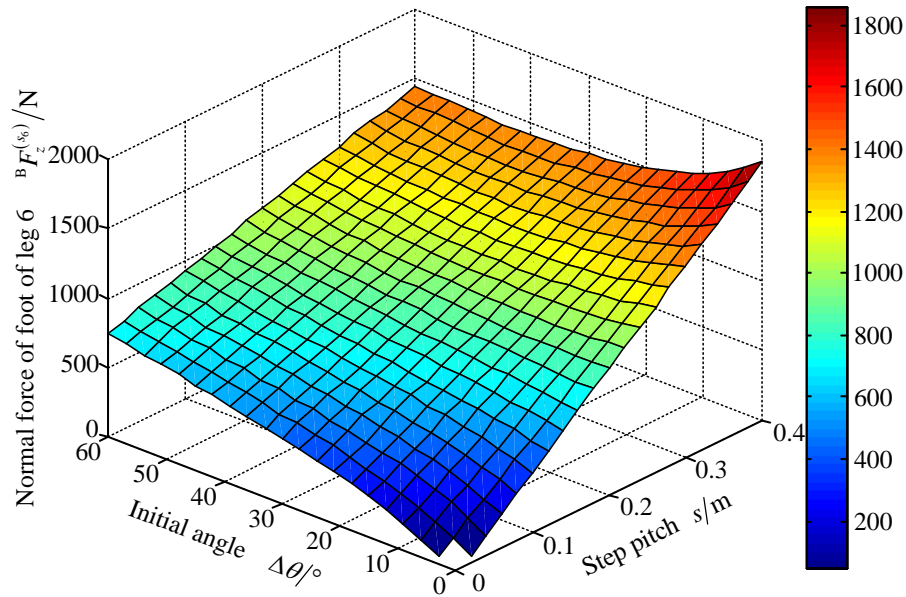


Fig. 8 Variable tendency chart of normal force of foot for leg 6 with changes in $\Delta\theta$ and s under ant-type tripod gait

- Based on Fig. 8, with the initial angle $\Delta\theta$ varying from 0° to 60° ; it shows that the variable tendency of the normal force of the foot overall presents from a decrease to augmentation for the leg 6, when the step pitch s is between 0.2 m to 0.4 m.
- The normal force of the foot of leg 6 gradually increases when the step pitch s is between 0 m to 0.2 m.
- It can be found that the normal force of the foot increases overall for leg 6, when the initial angle $\Delta\theta$ is a fixed value and the range of step pitch s is from 0 m to 0.4 m.

4 Force Theoretical Analysis of Foot under Gait of Robot

- According to Fig. 6, Fig. 7, and Fig. 8, the curves of the maximum normal forces of feet are obtained for legs 2, 4, and 6 with the varying of the initial angle $\Delta\theta$ and step pitch s . When $s = 0.4$ m and $20^\circ \leq \Delta\theta \leq 60^\circ$; the curves of the maximum normal forces of feet are shown in Fig.9.
- When $0.1 \text{ m} \leq s \leq 0.4 \text{ m}$ and $\Delta\theta = 20^\circ$; the curves of the maximum normal forces of feet are shown in Fig. 10.
- When $0.1 \text{ m} \leq s \leq 0.4 \text{ m}$ and $\Delta\theta=60^\circ$; the curves of the maximum normal forces of feet are shown in Fig. 11.

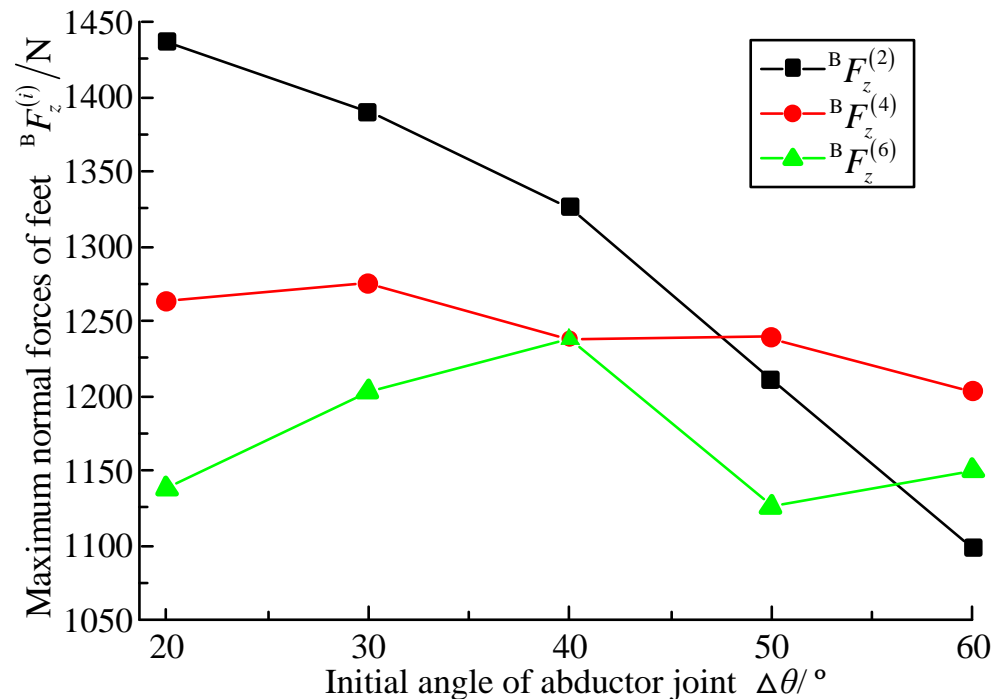


Fig. 9 Curves of maximum normal forces of feet under $s=0.4$ m, $20^\circ \leq \Delta\theta \leq 60^\circ$; and ant-type tripod gait

4 Force Theoretical Analysis of Foot under Gait of Robot

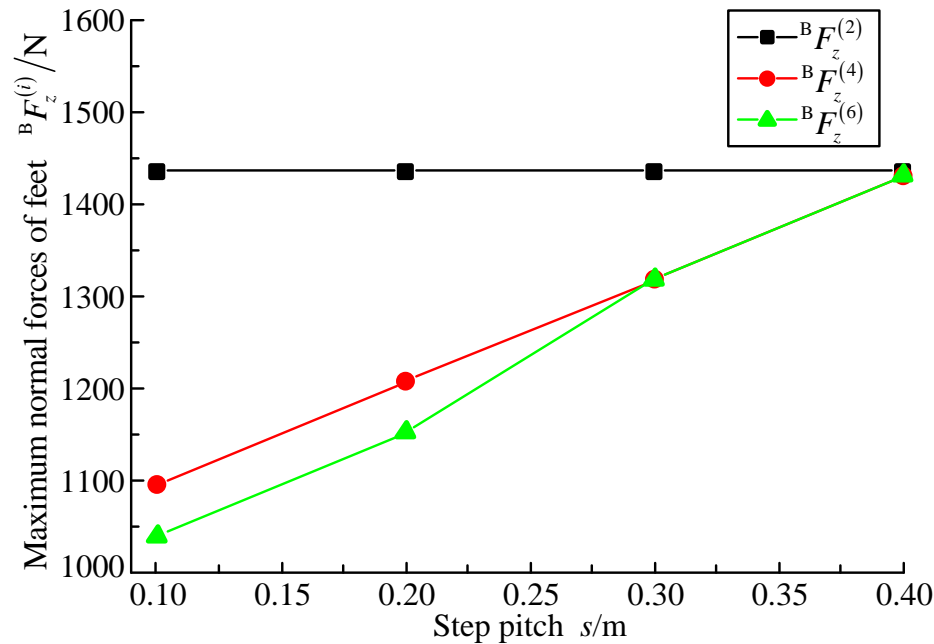


Fig. 10 Curves of maximum normal forces of feet under $0.1 \text{ m} \leq s \leq 0.4 \text{ m}$, $\Delta\theta=20^\circ$, and ant-type tripod gait

□ According to Fig. 9, when the step pitch s is 0.3 m and the initial angle $\Delta\theta$ varies from 20° to 60° , it can be found that the maximum normal force of the foot of leg 2 gradually reduces, and the maximum normal forces of feet are from augmentation to a decrease for the legs 4 and 6.

□ Based on Fig. 10, when the step pitch s varies from 0.1 m to 0.4 m and the initial angle $\Delta\theta$ is 20° , it shows that the maximum normal force of the foot is a constant for the leg 2, and the maximum normal forces of feet gradually decreases for the legs 4 and 6.

4 Force Theoretical Analysis of Foot under Gait of Robot

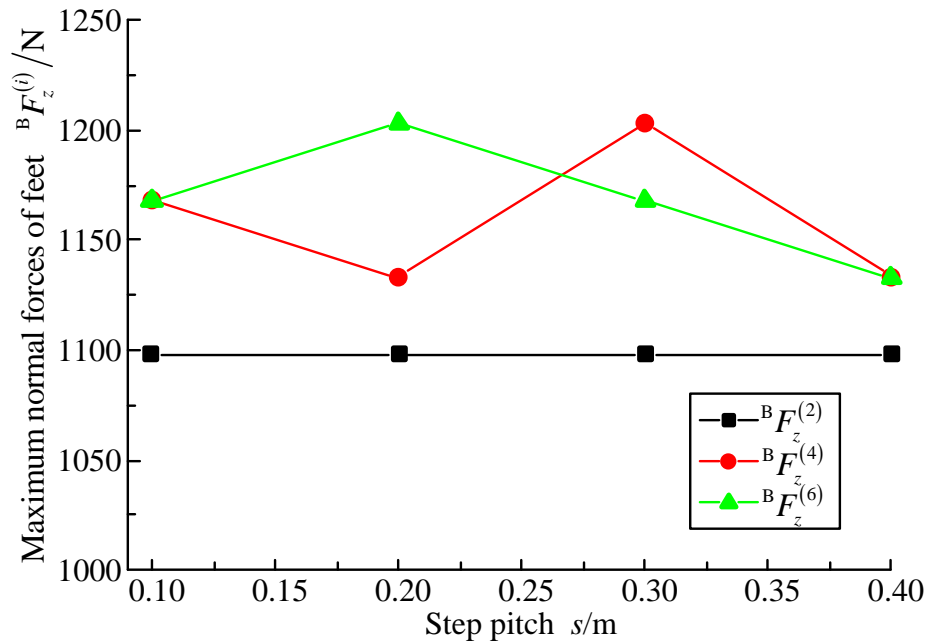


Fig. 11 Curves of maximum normal forces of feet under $0.1 \text{ m} \leq s \leq 0.4 \text{ m}$, $\Delta\theta = 60^\circ$, ant-type tripod gait

- According to Fig. 11, when the step pitch s changes from 0.1 m to 0.4 m and the initial angle $\Delta\theta$ is 60° , it can be found that the maximum normal force of the foot remains constant for the leg 2, the maximum normal force of the foot first decreases, then increases, and finally decreases for leg 4, and the maximum normal force of the foot of leg 6 varies from augmentation to a decrease.

4 Force Theoretical Analysis of Foot under Gait of Robot

4.2 Theoretical Analysis of Normal Force of Foot under Crab-Type Tripod

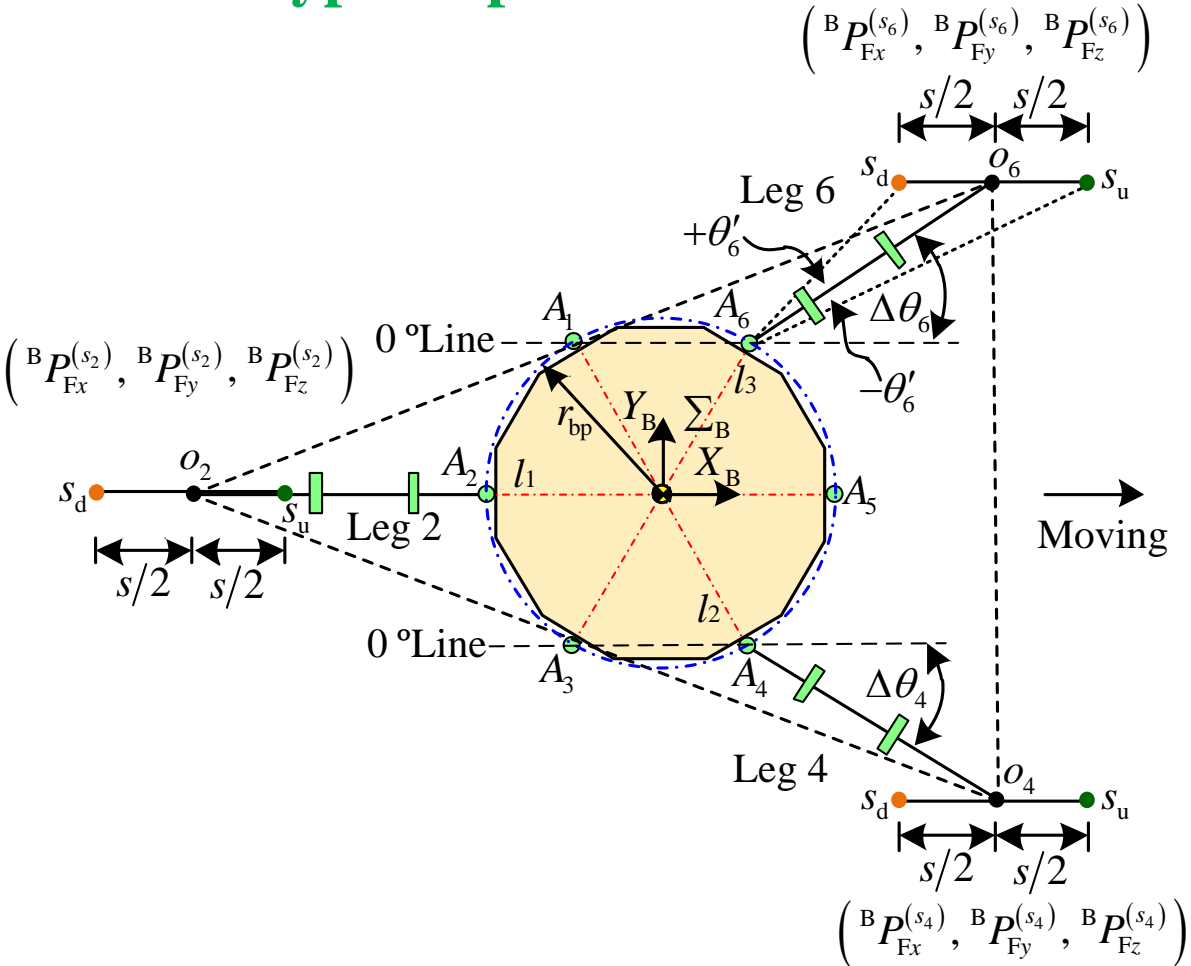


Fig. 12 Support phase of heavy-duty six-legged under crab-type tripod gait

4 Force Theoretical Analysis of Foot under Gait of Robot

Based on Fig. 12, the feet's coordinate in the support phase can be obtained along the y direction of the body coordinate system.

$$\begin{cases} {}^B P_{Fy}^{(s_2)} = 0 \\ {}^B P_{Fy}^{(s_4)} = -\left(r_{bp} \sin 60^\circ + L'_{P4} \sin(\Delta\theta_4)\right) \\ {}^B P_{Fy}^{(s_6)} = \left(r_{bp} \sin 60^\circ + L'_{P6} \sin(\Delta\theta_6)\right) \end{cases} \quad (17)$$

The support points of the legs respectively move from the upper point s_u to the lower point s_d . The coordinates of the feet at the lower point s_d can be respectively obtained along the x direction in the body coordinate system.

$$\begin{cases} {}^B P_{Fx}^{(s_2)} = -\left(r_{bp} + L'_{P2}\right) - \frac{s}{2} \\ {}^B P_{Fx}^{(s_4)} = r_{bp} \cos 60^\circ + L'_{P4} \cos(\Delta\theta_4) - \frac{s}{2} \\ {}^B P_{Fx}^{(s_6)} = r_{bp} \cos 60^\circ + L'_{P6} \cos(\Delta\theta_6) - \frac{s}{2} \end{cases} \quad (18)$$

4 Force Theoretical Analysis of Foot under Gait of Robot

Eq. (17) and Eq. (18) can be substituted into Eq. (12), and the mathematical models of the normal forces of the feet can be respectively deduced for legs 2, 4, and 6. Then

$$\left\{ \begin{array}{l} {}^B F_z^{(s_2)} = \frac{(r_{bp} + 2L'_{PS} \cos(\Delta\theta) - s)(m_L g + m_R g)}{3r_{bp} + 2L'_{PS} + 2L'_{PS} \cos(\Delta\theta)} \\ {}^B F_z^{(s_4)} = \frac{(r_{bp} + L'_{PS} + s/2)(m_L g + m_R g)}{3r_{bp} + 2L'_{PS} + 2L'_{PS} \cos(\Delta\theta)} \\ {}^B F_z^{(s_6)} = \frac{(r_{bp} + L'_{PS} + s/2)(m_L g + m_R g)}{3r_{bp} + 2L'_{PS} + 2L'_{PS} \cos(\Delta\theta)} \end{array} \right. \quad (19)$$

4 Force Theoretical Analysis of Foot under Gait of Robot

- The step pitch s , height h of the body, and initial offset L'_{PS} are respectively set by 0.4 m, 0.5 m, and 0.68 m for the heavy-duty six-legged robot, when the feet in support phase move from the upper point s_u to the lower point s_d .
- The ranges of the initial angles of abductor joints are from 0° to 60° for legs 1, 3, 4, and 6. The radius r_{bp} of body is introduced into Eq. (19).
- The MATLAB software is employed to analyze the normal forces of the feet in the support phase under the ant-type tripod gait.
- The variable tendency charts of the normal forces of the feet are obtained and respectively shown in Fig. 13 and Fig. 14 for legs 2, 4, and 6.

4 Force Theoretical Analysis of Foot under Gait of Robot

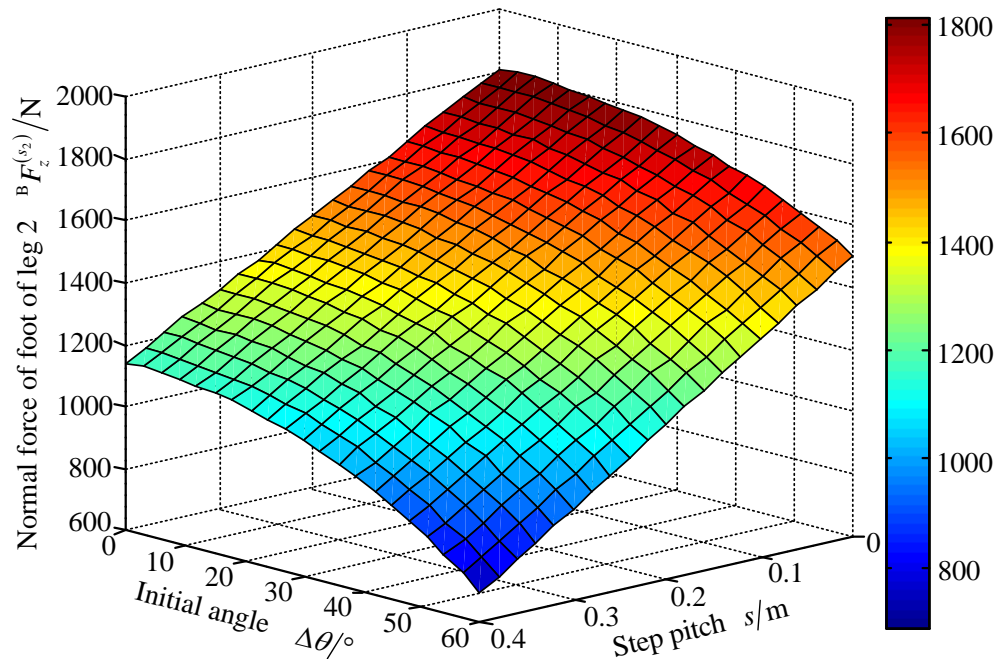


Fig. 13 Variable tendency chart of normal force of foot for leg 2 with changes in $\Delta\theta$ and s under crab-type tripod gait

- Based on Fig. 13, it shows that the normal force of the foot decreases for leg 2, when the step pitch s is a fixed value and the range of initial angle $\Delta\theta$ is from 0° to 60° ; or when the initial angle $\Delta\theta$ is a fixed value and the range of step pitch s is from 0 m to 0.4 m.
- The foot's minimum normal force of leg 2 is 691.1 N, when the step pitch s is 0.4 m and the initial angle $\Delta\theta$ is 60° .

4 Force Theoretical Analysis of Foot under Gait of Robot

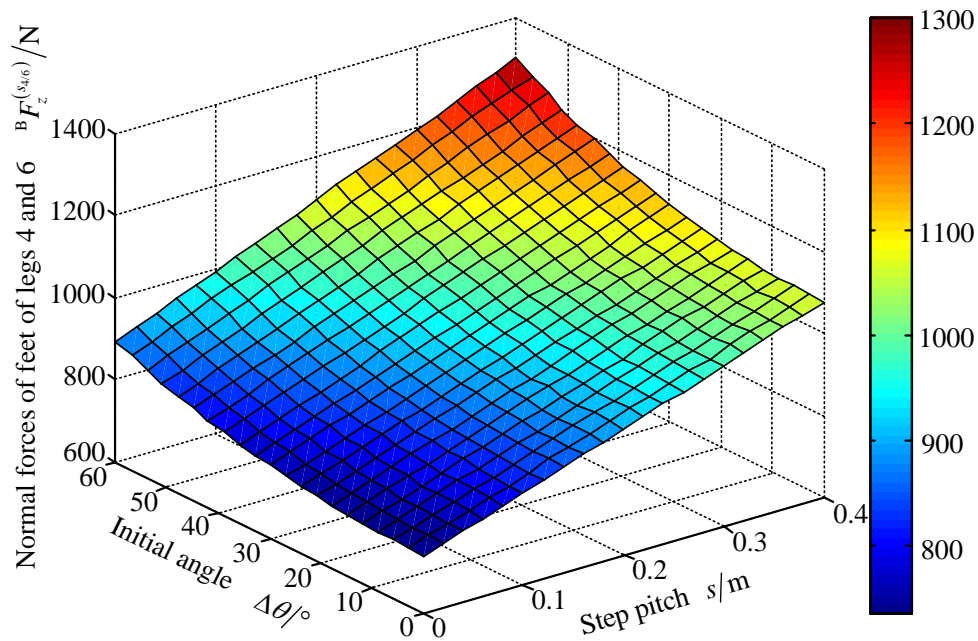


Fig. 14 Variable tendency charts of normal forces of feet for legs 4 and 6 with changes in $\Delta\theta$ and s under crab-type tripod gait

- Based on Fig. 14, it shows that the normal forces of legs 4 and 6 increase, when the step pitch s is a fixed value and the range of initial angle $\Delta\theta$ is from 0° to 60° ; or when the initial angle $\Delta\theta$ is a fixed value and the range of step pitch s is from 0 m to 0.4 m.
- The minimum normal forces of feet are 739.2 N for leg 4 and leg 6, when the step pitch s and initial angle $\Delta\theta$ are 0 m and 0° , respectively.

4 Force Theoretical Analysis of Foot under Gait of Robot

- Based on Fig. 13 and Fig. 14, the curves of the maximum normal forces of feet are respectively obtained for legs 2, 4, and 6 with the initial angle $\Delta\theta$ and step pitch s varying.
- When $s = 0.2$ m and $0^\circ \leq \Delta\theta \leq 60^\circ$, the curves of the maximum normal forces of feet are shown in Fig. 15.
- When 0.05 m $\leq s \leq 0.2$ m and $\Delta\theta = 0^\circ$, the curves of the maximum normal forces of feet are shown in Fig. 16.
- When 0.1 m $\leq s \leq 0.4$ m and $\Delta\theta = 60^\circ$, the curves of the maximum normal forces of feet are shown in Fig. 17.

4 Force Theoretical Analysis of Foot under Gait of Robot

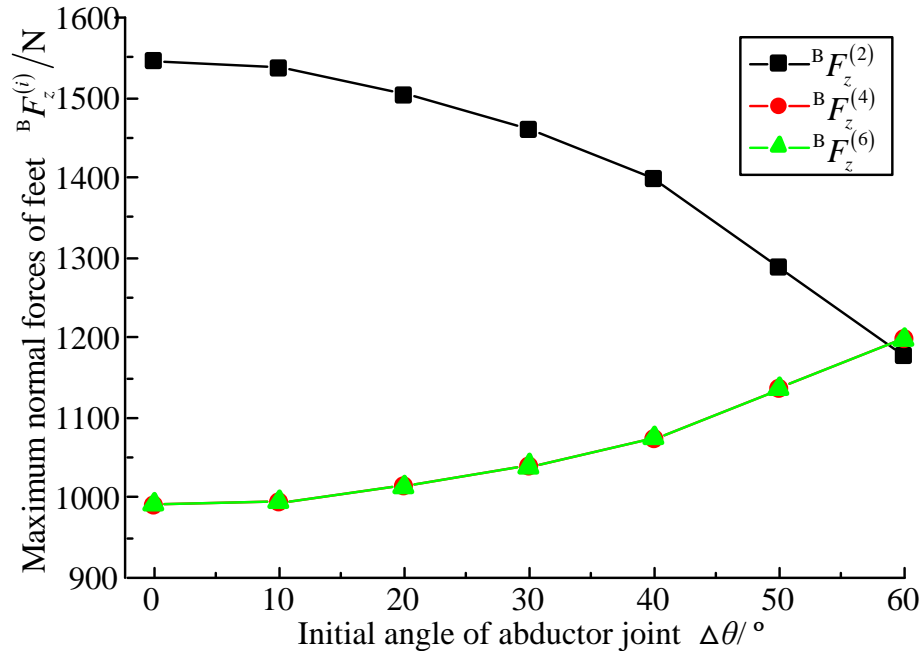


Fig. 15 Curves of maximum normal forces of feet under $s=0.2$ m, $0 \leq \Delta\theta \leq 60^\circ$, and crab-type tripod gait

- Based on Fig. 15, when the step pitch s is 0.2 m and the initial angle $\Delta\theta$ varies from 0° to 60° , it shows that the maximum normal force of the foot gradually decreases for leg 2, and gradually increases for leg 4 and leg 6, respectively.
- The maximum normal forces of the feet are equal to each other for legs 2, 4, and 6, when the initial angle $\Delta\theta$ is 60° .

4 Force Theoretical Analysis of Foot under Gait of Robot

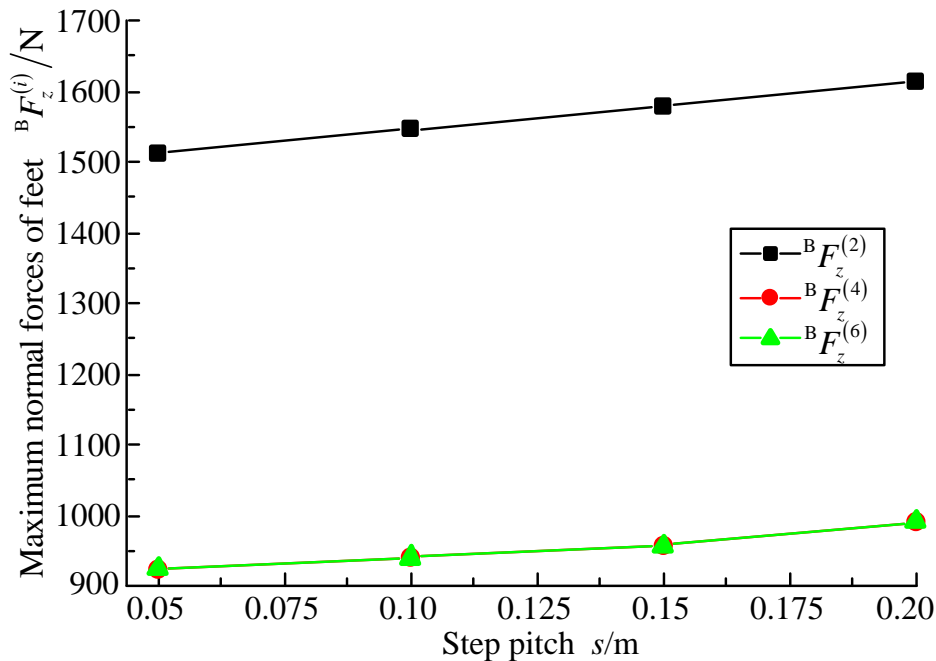


Fig. 16 Curves of maximum normal forces of feet under $0.05 \text{ m} \leq s \leq 0.2 \text{ m}$, $\Delta\theta=0^\circ$; crab-type tripod gait

- According to Fig. 16, when the initial angle $\Delta\theta$ is 0° and the step pitch s varies from 0.05 m to 0.2 m, it shows that the maximum normal forces of feet gradually increase for legs 2, 4, and 6.
- The curves of the maximum normal forces of the feet are the same for leg 4 and leg 6.

4 Force Theoretical Analysis of Foot under Gait of Robot

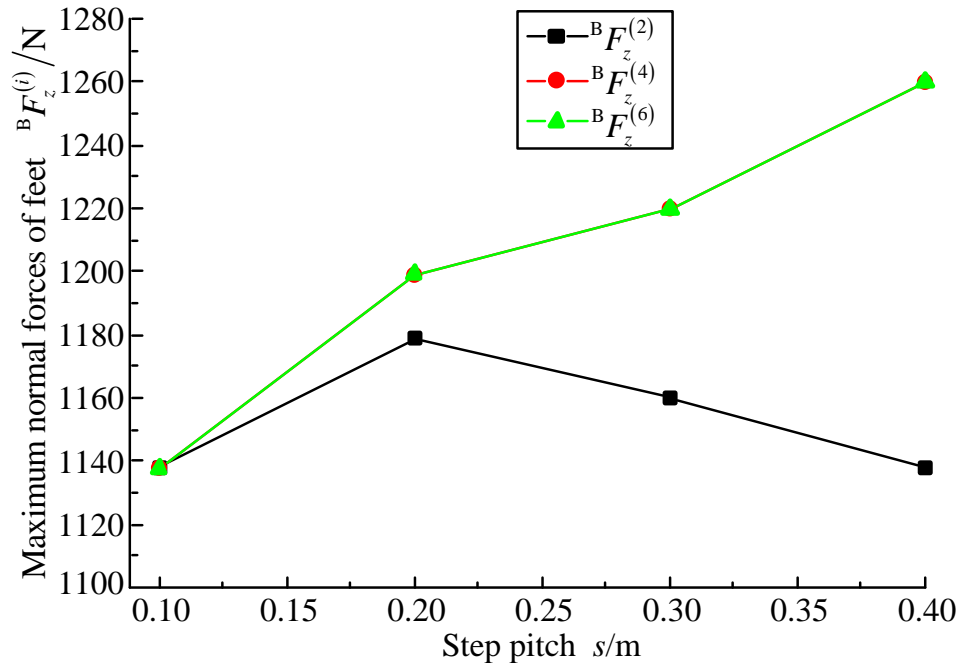


Fig. 17 Curves of maximum normal forces of feet under $0.1 \text{ m} \leq s \leq 0.4 \text{ m}$, $\Delta\theta=60^\circ$; crab-type tripod gait

- Based on Fig. 17, when the initial angle $\Delta\theta$ is 60° and the step pitch s varies from 0.1 m to 0.4 m, it can be concluded that the variable tendency of the maximum normal force of the foot augments then decreases for leg 2.
- The maximum normal forces of the feet are equal and gradually increase with the change of the step pitch for leg 4 and leg 6.

5 Force Experimental Analysis of Foot under Robotic Gait

The prototype of electrically driven heavy-duty six-legged robot was developed. The walking experiments of prototype are implemented under four kinds of typical tripod gaits on a flat ground. The variable tendency of the maximum normal force of the foot of leg i can be obtained.



Fig. 18 Walking experiments of mixture-type II walking mode

5 Force Experimental Analysis of Foot under Robotic Gait

5.1 Force Experimental Analysis of Foot under Ant-Type Tripod Gait

5.1.1 Changing initial angle $\Delta\theta_i$

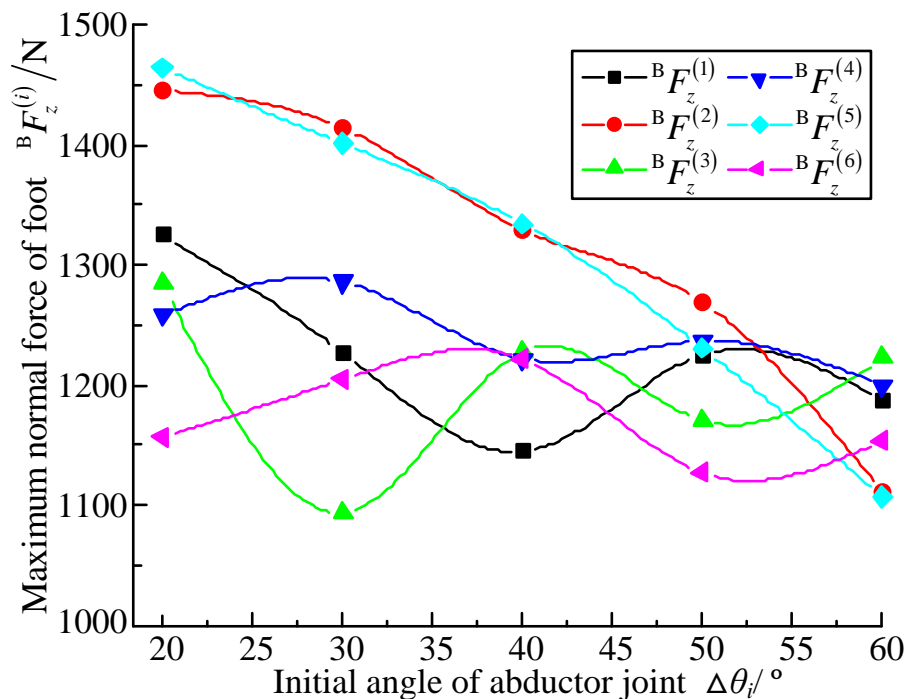


Fig. 19 Variable tendencies of maximum normal forces of feet with change in initial angle under ant-type tripod gait

- Fig. 19 shows that the maximum normal forces for the feet of leg 2 and leg 5 gradually decrease with the change in the initial angle, and their variable tendencies are equal. When the initial angle is 60° , the minimum difference exists among the maximum normal forces of the feet.
- Based on Fig. 9 and Fig. 19, it is concluded that the variable tendencies of the feet's maximum normal forces are respectively corresponding to the same for legs 2, 4, and 6, when the step pitch is 0.3 m and the initial angle varies from 20° to 60° .

5 Force Experimental Analysis of Foot under Robotic Gait

5.1.2 Changing step pitch s

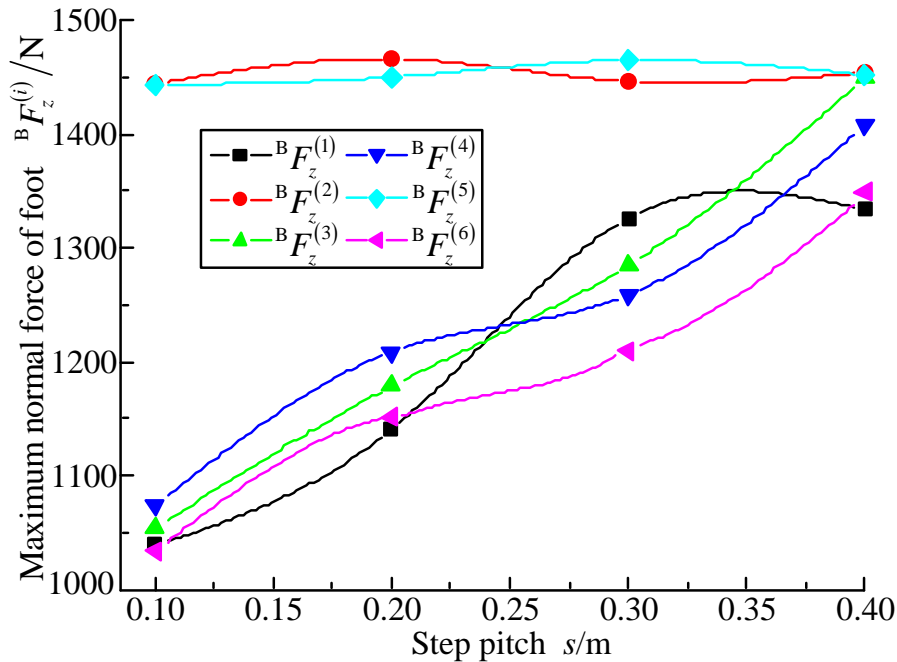


Fig. 20 Variable tendencies of maximum normal forces of feet with change in step pitch under ant-type tripod gait

- Based on Fig. 20, with the step pitch varying from 0.1 m to 0.4 m, it is concluded that the curves of the maximum normal forces of feet keep stable for leg 2 and leg 5, and they are over other curves. It can be found that the force distribution is easier to realize when the step pitch has a larger value.
- Based on Fig.10 and Fig.20, it can also be concluded that the variable tendencies of the maximum normal forces of the feet are respectively corresponding to the same for legs 2, 4, and 6, when the initial angle is 20° and the step pitch varies from 0.1 m to 0.4 m.

5 Force Experimental Analysis of Foot under Robotic Gait

5.2 Force Experimental Analysis of Foot under Crab-Type Tripod Gait

5.2.1 Changing initial angle $\Delta\theta_i$

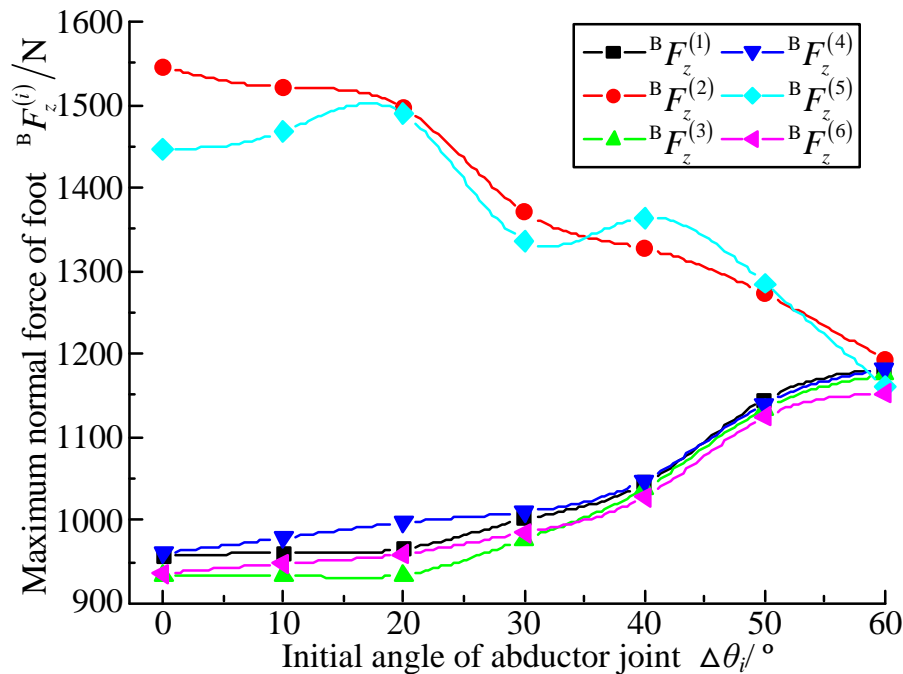


Fig. 21 Variable tendencies of maximum normal forces of feet with change in initial angle under crab-type tripod gait

Based on Fig. 21, it shows that the curves of the maximum normal forces of the feet present a gradually downward trend for leg 2 and leg 5, and gradually rising trends for the other legs, with the initial angle varying from 0° to 60° . The maximum normal forces of the feet are approximately equal to each other, when the initial angle is 60° .

Based on Fig.15 and Fig. 21, it can be found that the variable tendencies of the maximum normal forces of the feet are respectively corresponding to the same for legs 2, 4, and 6, when the step pitch is 0.2 m and the initial angle varies from 0° to 60° .

5 Force Experimental Analysis of Foot under Robotic Gait

5.2.2 Changing step pitch s

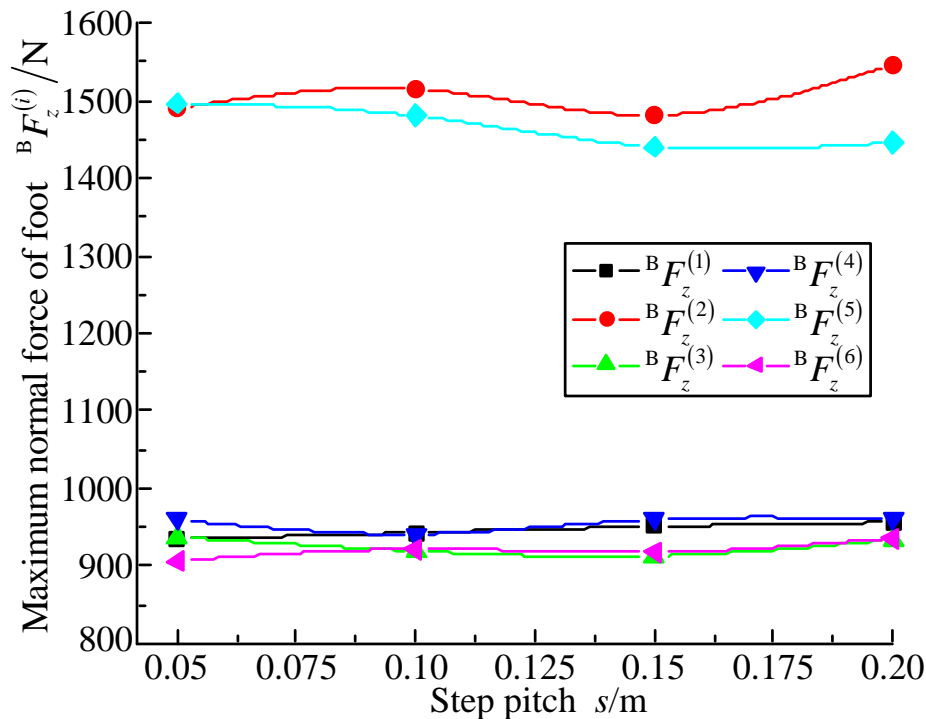


Fig. 22 Variable tendencies of maximum normal forces of feet with change in step pitch under crab-type tripod gait

- Based on Fig. 22, with the step pitch varying, it can be concluded that the curves of the maximum normal forces of the feet are mostly uniform for leg 2 and leg 5, for leg 3 and leg 4, and for leg 2 and leg 5, respectively.
- Based on Fig.16 and Fig.22, it can be concluded that the variable tendencies of maximum normal forces of the feet are respectively corresponding to the same for legs 2, 4, and 6, when the initial angle is 0° and the step pitch varies from 0.05 m to 0.2 m.

5 Force Experimental Analysis of Foot under Robotic Gait

5.3 Force Experimental Analysis of Foot under Mixture-type I Tripod Gait

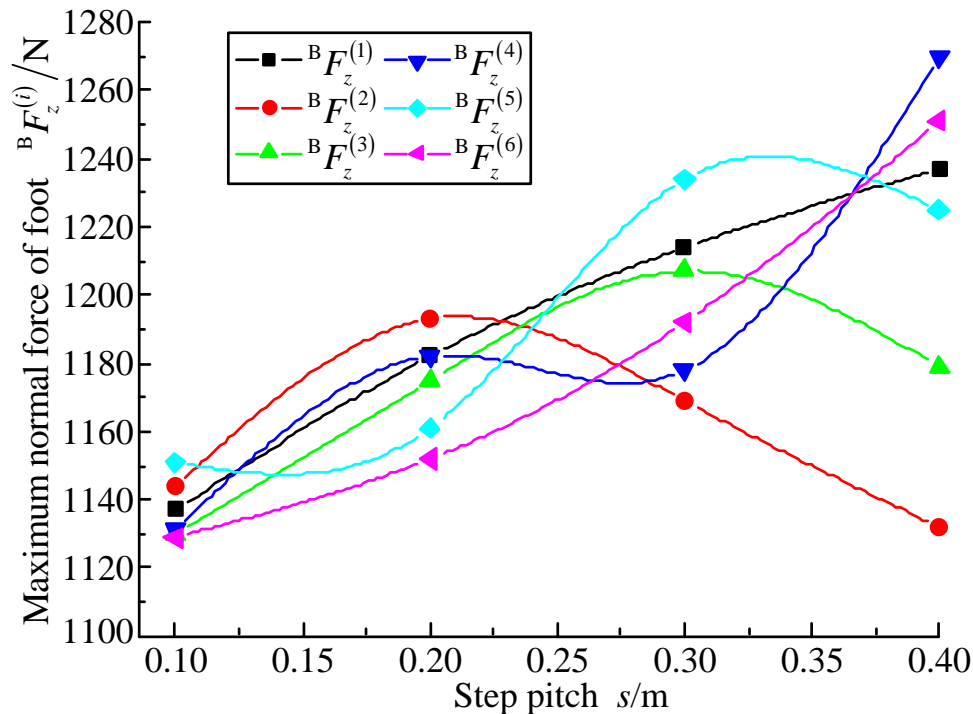


Fig. 23 Variable tendencies of maximum normal forces of feet with change in step pitch under mixture-type I tripod gait

- Based on Fig. 23, it can be concluded that the deviations of maximum normal forces of the feet become larger with the step pitch increasing from 0.1 m to 0.4 m.
- According to Fig. 17 and Fig. 23, it can be found that the variable tendencies of maximum normal forces of the feet correspond uniformly for legs 2, 4, and 6, respectively, when the initial angle is 60° and the step pitch ranges between 0.1 m to 0.4 m.

5 Force Experimental Analysis of Foot under Robotic Gait

5.4 Force Experimental Analysis of Foot under Mixture-Type II Tripod Gait

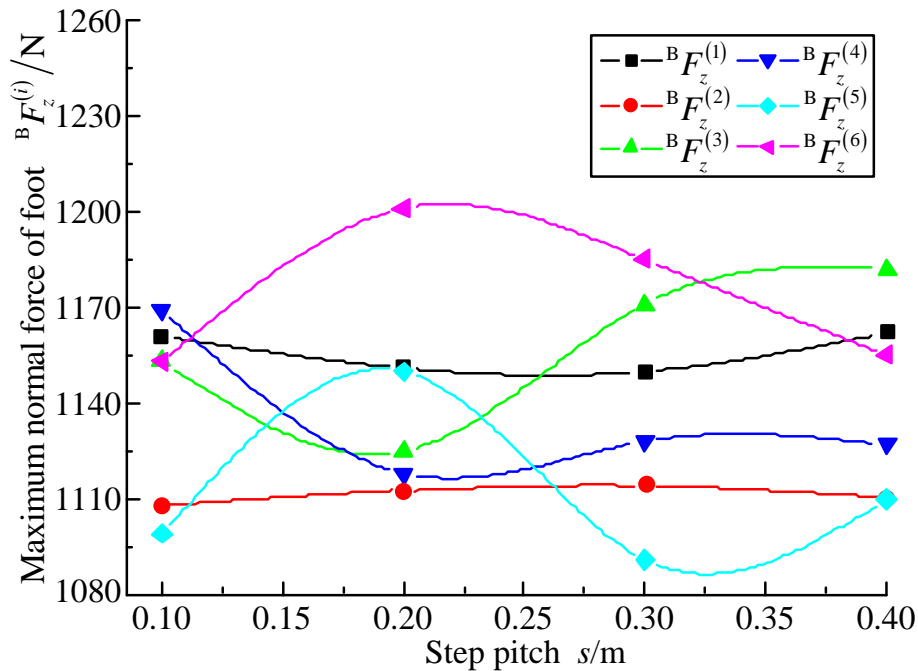


Fig. 24 Variable tendencies of maximum normal forces of feet with change in step pitch under mixture-type II tripod gait

- Based on Fig. 24, with the step pitch ranging from 0.1 m to 0.4 m, it can be concluded that the curve of the maximum normal force of the foot approximately keeps stable for leg 2. The variable tendency of the maximum normal force of foot presents from decrease to augmentation for leg 4; the variable tendency shows adverse to leg 6's.
- According to Fig.11 and Fig.24, it can be found that the variable tendencies of the maximum normal forces of the feet are respectively corresponding to the same for legs 2, 4, and 6, when the initial angle is 60° and the step pitch ranges between 0.1 m to 0.4 m.

5 Force Experimental Analysis of Foot under Robotic Gait

5.5 Amplitude Interval Analysis of Normal Force of Foot under Gait of Robot

- Based on the analysis above, it can be obtained that the results of theoretical and experimental data keep consistent in the aspect of the maximum normal force of the foot.
- Hence, it can be concluded that the reasonableness and correctness can be respectively obtained for the force theoretical analysis of the foot and experimental data under four kinds of typical tripod gaits of heavy-duty six-legged robots.
- Based on Fig.19-Fig. 24, the ranges of maximum normal forces of the feet are respectively obtained under four kinds of typical tripod gaits, as shown in Table 1.

5 Force Experimental Analysis of Foot under Robotic Gait

Table 1 Ranges of maximum normal forces of feet under four kinds of typical tripod gaits

Walking modes	Ranges of maximum normal forces of feet	
	R_F / N	
	Change in initial angle	Change in step pitch
Ant type	370	432
Crab type	614.5	638.4
Mixture type I	—	141
Mixture type II	—	157

- It can be concluded that the mixture-type I and mixture-type II walking modes are better than the ant type and crab type in the aspect of the force distribution and stability.
- It can be obtained that the mixture-type II walking mode is the best and should be preferentially employed for the heavy-duty six-legged robot with the consideration of walking speed.

6 Conclusions

- Four kinds of typical walking modes are obtained based on the configuration of root. The variable tendency charts of normal forces of the feet are described with the changes in the initial angle and step pitch by performing the theoretical analysis of static foot force.
- According to the walking experiments of robot prototype under four kinds of typical tripod gaits, the variable tendencies of the maximum normal forces of feet are respectively obtained with the changes in the initial angle and step pitch. The comparison results show that the theoretical and experimental data are in the same trend under the same variable and same walking mode of the tripod gait.
- The optimal walking mode, the mixture-type II walking mode, is confirmed, and it is firstly recommended for the electrically driven heavy-duty six-legged robot in view of its excellent characteristics in walking speed, stability, force distribution, and load ratio.

Acknowledgments

This work was supported by National Natural Science Foundation of China (Grant No. 51505335), National Natural Science Foundation of China (Grant No. 51275106), National Basic Research Program of China (973 Program, Grant No. 2013CB035502)

Biographical notes

- **Zhen Liu**, born in 1983, is currently a lecturer at *State Key Laboratory of Robotics and System, Harbin Institute of Technology, China*. He received his PhD degree from *Harbin Institute of Technology, China*, in 2013. His research interests include planetary rover technology and aerospace mechanisms and control.

Tel: +86-451-86402037-801; E-mail: liuzhen_hit@163.com

- **Hong-Chao Zhuang**, born in 1982, is currently a lecturer at *College of Mechanical Engineering, Tianjin University of Technology and Education, China*. He received his PhD degree from *Harbin Institute of Technology, China*, in 2015. His research interests include special robot systems and intelligent robotics.

Tel: +86-451-86402037-801; E-mail: zhuanghongchao_hit@163.com

- **Hai-bo Gao**, born in 1970, is currently a professor and a supervisor for PhD candidates at *State Key Laboratory of Robotics and System, Harbin Institute of Technology, China*. He received his PhD degree from *Harbin Institute of Technology, China*, in 2004. His research interests include special robot systems and aerospace mechanisms and control.

Tel: +86-451-86402037-801; E-mail: gaohaibo@hit.edu.cn

Biographical notes

- **Zong-Quan Deng**, born in 1956, is currently a professor and a supervisor for PhD candidates at *Harbin Institute of Technology, China*. He received his master's degree from *Harbin Institute of Technology, China*, in 1984. His research interests include planetary rover technology and aerospace mechanisms and control.

Tel: +86-451-86413857; E-mail: dengzq@hit.edu.cn

- **Liang Ding**, born in 1980, is currently a professor and a supervisor for PhD candidates at *State Key Laboratory of Robotics and System, Harbin Institute of Technology, China*. He received his PhD degree from *Harbin Institute of Technology, China*, in 2009. His research interests include planetary rover technology and aerospace mechanisms and control. Tel: +86-451-86402037-801; E-mail: liangding@hit.edu.cn

Thank you!